IFSCC 2025 full paper (IFSCC2025-736)

"Development of an in-vitro setup using 'Skinsight™' for the evaluation of the skin tightness delay effects"

Kyungsup Han[1,*], Minkyung Kwon[1], Jun Min Suh[2], Moonjeong Bok[1], Sung Yeon Cho[1], Myeongjin Goh[1], Jin Nam[1], Won-Seok Park[1] and Jeehwan Kim[2]

[1] R&I center, Amorepacific , Yongiin-si, Korea, South; [2] Mechanical Engineering, Massachusetts Institute of Technology, Massachusetts, United States

1. Introduction

In recent days, there has been an increased demand for cosmetics that emphasize inner-skin hydration and the improvement of skin dryness. Consumers are looking for immediate relief from the uncomfortable feeling of dryness and anti-aging effects from a preventative perspective. The initial physical change and sensory signal associated with insufficient inner-skin hydration can be characterized by skin tightness [1]. The prolonged experience of skin tightness may result in a reduction in skin elasticity with a clear perception of skin tension. Recurring experience of the skin tightness can raise the possibility of irreversible skin aging which is a huge concern in general population. Therefore, direct and quantitative measurement of skin tightness can provide significant insights into the contributing factors behind changes in skin physiology and structural damages, whether caused by inner-skin moisture levels or other potential factors. This quantitative evaluation of human-subjective sensory experiences can be beneficial in demonstrating the immediate relieving effects of cosmetic products to potential consumers. Nevertheless, detection of very minute changes occurring in the skin dermis necessitates extremely sensitive and precise sensor technologies that can directly measure the changes. To the author's best knowledge, there have been no commercially available devices in the market that can directly and quantitatively measure skin tightness. Although there have been several indirect measurement tools that are clinically applicable like Raman spectroscopy, TEWL, Skicon®, Corneometer, or tape stripping, no direct measurement methodology exists to date [2-6]. For example, Raman spectroscopy and Skicon® collects inner-skin moisture data to indirectly predict skin-tightness, but they lack the ability to provide intuitive and reliable skin tightness information to the users. The research team at Stanford University, in collaboration with L'Oréal, revealed a correlation between the perception of skin tightness and biomechanical changes (i.e. alterations in elasticity and skin moisture levels) that affect tactile receptors in the basal layer of the skin [1]. They combined

in-vitro tests measuring skin drying stress in the stratum corneum (SC) using finite element analysis (FEA) with human surveys to identify this correlation. However, this method involves artificially drying the skin surface and therefore does not reflect the natural conditions of skin moisture evaporation. Furthermore, the low elasticity of the SC influences overall skin model movement, rendering it less representative of inner-skin tightness. Consequently, the development of a sensor capable of directly measuring skin tightness is imperative. Recently, a collaboration between Amorepacific and MIT resulted in the development of an electronic skin platform equipped with four different sensors, including an ultra-sensitive strain sensor (Skinsight™) that facilitates direct measurement of skin tightness [7]. In this study, an in vitro setup is proposed for efficiently evaluating the tightness delay effects of cosmetic products by connecting Skinsight™ to human ex-vivo skin (skin specimen). This in vitro test setup has been demonstrated to measure skin tightness with a high precision comparable to that achieved through the insertion of sensors into the skin. Furthermore, the additional objectives of this study are as follows: first, to evaluate the differences in the tightness-delaying effects of cosmetic products depending on whether they penetrate beyond the SC; and second, to determine whether selection criteria for humectants can be differentiated at the raw material level based on their effects on skin tightness.

2. Materials and Methods

2.1. Working principle

In order to measure and quantify skin tightness, a highly sensitive sensor capable of detecting extremely small changes on skin surfaces is essential. The developed ultra-sensitive strain sensor, Skinsight™, is a piezotronic sensor based on piezoelectric materials and potential barrier engineering. Piezoelectric materials generate voltage in response to external mechanical stimuli, and engineered potential barriers—specifically Schottky barriers—can utilize this piezoelectric voltage to modulate electron tunneling across the barriers, resulting in changes in conductance. In Skinsight™, zinc oxide (ZnO) is used as the piezoelectric material, and hafnium oxide (HfO_2) is employed as the Schottky barrier material. The thickness of the HfO_2 layer is carefully controlled to maximize strain sensitivity. Skinsight™ is fabricated using conventional semiconductor manufacturing processes, and the overall device thickness is as thin as 24 μm, making it flexible enough to conform to the skin’s contours. Additionally, an auxetic dumbbell hole pattern is applied across the entire device area to enable even more conformal attachment, minimizing any potential signal damping between the skin and the device. The dimensions of the auxetic dumbbell hole pattern are designed based on those of sweat pores, to prevent the accumulation of sweat or other skin byproducts at the skin-device interface, thereby facilitating precise data collection. Besides sensor development, since changes in skin tightness are extremely subtle and the corresponding sensor signals are expected to be very small, an appropriate measurement setup and carefully designed protocols are also essential.

2.2. Fabrication of Skinsight™

The fabrication of Skinsight™ starts with a highly doped Si wafer with a sheet resistance lower than 0.001 Ω·cm. Thermal evaporation of titanium (Ti) and aluminum (Al) is then conducted. Ti is used as an adhesive layer, and Al serves as a sacrificial layer that will be

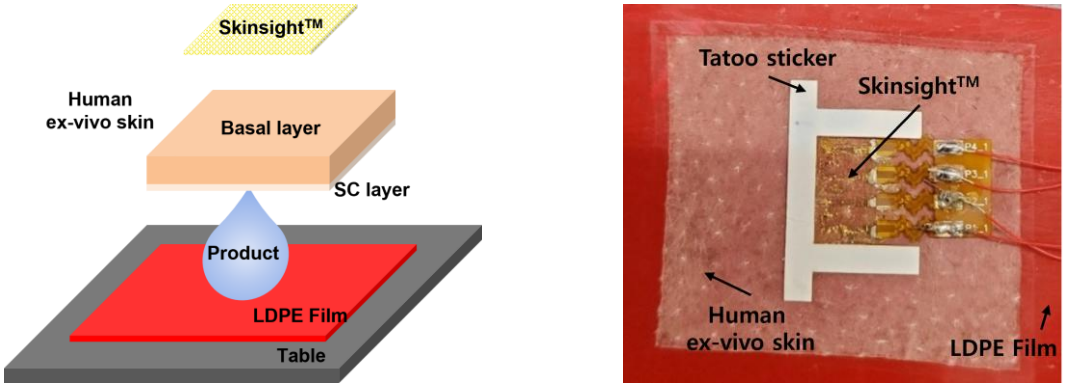

(**a**) (**b**)

Figure 1. (a) Schematic diagram of the in-vitro setup showing the stacked configuration from top to bottom: sensor (Skinsight™), human ex-vivo skin epidermis model, cosmetic product, and LDPE film; (b) Photograph of the actual test sample illustrating the assembled configuration.

dissolved in a later step to release Skinsight™ from the wafer. After the deposition, (3-Aminopropyl)triethoxysilane (APTES, MilliporeSigma, USA), diluted in distilled water (1%), is spin-coated onto the Al/Ti/Si wafer at 4000 rpm and baked at 115 °C for 1 min. Then, 4,4′-Methylenebis(N,N-diglycidylaniline) (MilliporeSigma, USA) is spin-coated at 6000 rpm and baked at 250 °C for 1 hr to cure into polyimide (PI) with an expected thickness of 2 μm. On the cured PI, conventional photolithography followed by e-beam evaporation of chromium (Cr, 5 nm) and gold (Au, 100 nm) is carried out to form the interconnect layer, followed by a lift-off process. On the interconnect layer, atomic layer deposition (ALD) of HfO_2 (15 cycles), ZnO (600 cycles), and HfO_2 (20 cycles) is performed at 200 °C to fabricate the piezotronic sensor on the electrodes. After the deposition, another round of conventional photolithography is performed to define the active sensor area, and the unwanted regions are etched away using carbon fluoride (CF_4) dry etching for HfO_2 and hydrochloric acid (HCl) wet etching for ZnO, respectively. Then, another PI layer (2 μm) is formed over the entire substrate by spin-coating at 5000 rpm and curing at 250 °C for 1 hr. It should be noted that while the bottom PI was spin-coated at 6000 rpm, the top PI was spin-coated at 5000 rpm to position the piezotronic sensors slightly off the neutral mechanical plane (NMP), thereby enabling effective strain detection. As a final step, auxetic dumbbell hole patterns are fabricated by reactive ion etching (O_2, 100 W, 1 hr) using thermally evaporated copper (Cu, 40 nm) as a hard mask after photolithography.

The separation of Skinsight™ from the Si wafer is enabled through the electrochemical dissolution of the Al layer. After spin-coating a poly(methyl methacrylate) (PMMA) layer (1500 rpm) on Skinsight™ and curing it (110 °C, 10 min) as a temporary handling layer, thermal release tape (TRT) is attached on top of the PMMA layer. Then, the backside of the Si wafer is scratched with sandpaper, and an electric wire is attached and completely sealed with PI tape to prevent exposure to the electrolyte during electrochemical release. The wire-connected wafer is immersed in an electrolyte solution (30 g NaCl in 750 ml distilled water), and electrochemical release is performed at 1.5 V for 20 hr using a Pt wire as the counter electrode. After 20 hr, the released device is collected, carefully washed with distilled water, and dried for further processing. On a separate Si wafer, a 20 μm-deep trench is fabricated by conventional photolithography of auxetic dumbbell hole patterns followed by deep reactive ion etching. After treating the Si trench with O_2 plasma and trichloro(1H,1H,2H,2H-

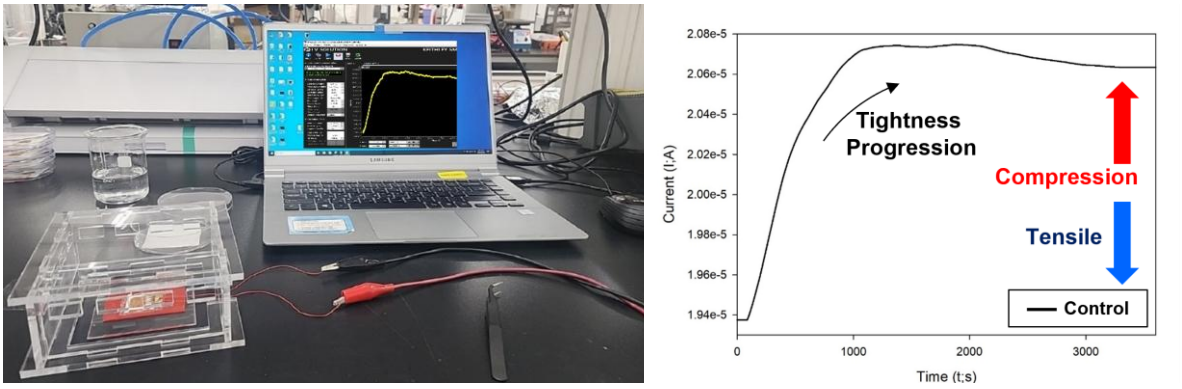

(**a**) (**b**)

Figure 2. (a) Experimental setup for real-time tightness measurement using a source meter, showing the test sample covered with a wind tunnel cover; (b) tative graph obtained from the source meter, illustrating the method for distinguishing compressive and tensile strain based on the direction of the current signal

perfluorooctyl)silane (MilliporeSigma, USA), polydimethylsiloxane (PDMS, Sylgard 184, Dow Inc., USA) is spin-coated after degassing in a vacuum desiccator. The mixing ratio of monomer to curing agent is 40:1 to achieve better adhesion and a lower elastic modulus. Skinsight™, still attached to the TRT, is carefully placed face-down on the uncured PDMS, aligning the auxetic dumbbell hole pattern with the Si trench by taking advantage of the TRT's semi-transparency. The PDMS is then cured at 80 °C under constant pressure (1.29 kPa) to ensure uniform through-hole formation in the Si trenches. Following the curing process, the Si trench is removed, and the TRT is detached by heating. The released structure is immersed in acetone and isopropyl alcohol to remove the PMMA layer and clean Skinsight™. The cleaned Skinsight™ is then scooped up and dried for further processing. Lastly, a temporary tattoo paper (Silhouette, USA) is cut to the dimensions of Skinsight™ and attached to the edge of the device to improve handling and facilitate skin application.

2.3. in-vitro setup & experimental protocol

The in-vitro setup has been developed to replicate the inner skin environment with respect to moisture absorption, evaporation, and subsequent tightness. The skin specimen was selected as the most suitable test system for simulating the above-mentioned environment [8]. Furthermore, an epidermal model of the skin with an exposed basal layer was selected to allow direct attachment of the sensor at the location where tightness signals occur, thereby ensuring signal measurement without loss. Fig. 1 represents the schematic diagram (a) and the actual assembly of the in-vitro setup (b), including the sensor, human ex-vivo skin, cosmetic product, and low-density polyethylene (LDPE) film. The skin specimen is comprised of the SC and the basal layer. The procedure involves attaching the skin sample in reverse order: first, the product is applied; then, the skin sample is placed with the SC facing downwards; and finally, Skinsight™ is attached to the basal layer side. This study simulates product absorption through the SC, while tightness changes are measured directly at the basal layer, where shrinkage occurs. In the final step of the in-vitro setup, a LDPE film is positioned at the bottom. In order to accurately measure shrinkage, the environment must allow shrinkage across the entire surface of the specimen. When the skin specimen is placed on most substrates and dried, the edges tend to curl due to moisture evaporation, while the center does not shrink well. To address this issue, it is necessary to cover the substrate with a material that has appropriate hydrophilicity relative to the skin specimen. This material absorbs

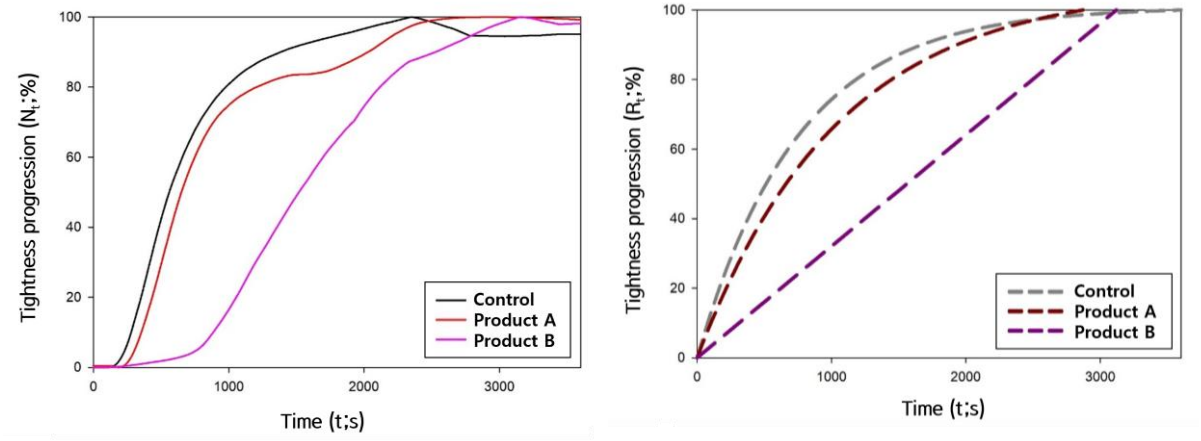

(**a**) (**b**)

Figure 3. Representative graphs of the data analysis process: (a) normalized result (N_t) graph comparing two different products; (b) regression analysis (R_t) graph (exponential rise to maximum) applied to the normalized data

moisture from the skin specimen, thereby maintaining a thin moisture layer during the shrinkage process. Consequently, LDPE film was used as the substrate to induce two-dimensional (2D) shrinkage without causing skin curling upon drying.

The experimental setup is shown in Fig. 2(a) and the detailed test protocol is as follows: First, attach the LDPE film to the PMMA/acrylic block. Remove the skin specimen from the freezer and thaw it for 3 min. Pipette 30 µL of the product onto the LDPE film, skipping this step for the negative control group. Tilt the thawed skin specimen and use a wipe to remove any water that has flowed out of the protective film. Next, remove the protective film covering only the SC (slit) side of the skin specimen, ensuring that the SC covers the product on the film. Then remove the protective film from the opposite side and absorb any surface moisture by touching it three times with a wipe, removing it immediately each time. Attach the skin specimen by placing the basal layer in contact with Skinsight™, with the wire positioned at the 3 o'clock position. Press lightly with the index finger to ensure that the strain sensor inside the tattoo sticker adheres properly. Cover the setup with the wind channel cover to protect the signal from wind interference and ensure the wire is not compressed. Complete the above steps within 5 min, then connect the wire to the source meter (Keithley 2400) and measure the current change for 60 min (3600 sec).

2.4. Data analysis

The well-designed data analysis method, including arrangement, normalization, and regression analysis, helps reduce errors and provides consistent trends for interpretation. Normalization is achieved by establishing a baseline of 0 % and an equilibrium of 100 % tightness progression, thereby facilitating standardized comparisons of the temporal development of tightness (Fig 3(a)). The application of an exponential rise-to-maximum regression model is a suitable approach for the observed tightness progression curves, where tightness increases exponentially towards a maximum value (Fig. 3(b)). The gradient of the regression curve has been shown to be a reliable indicator of the rate of tightness development. In order to address potential variations between sensors (Skinsight™) and the skin specimens, repeated testing (three times per sensor), averaging, and data point alignment through smoothing (interpolation) are employed to ensure reliable comparisons, especially for products with closely similar effects. The entire analysis process is automated using Sigma Plot. A quantitative

measurement of the tightness delay capacity can be obtained by comparing the area above the normalized tightness progression curve.

3. Results

3.1. Signal processing

The skin on the body is responsible for maintaining optimal hydration levels by facilitating the continuous evaporation of water and the supply of moisture from the bloodstream. It is evident that, owing to the interruption of the moisture supply to the skin specimen, a rapid loss of moisture occurs from the moment of thawing during the experiment. Consequently, the skin exhibits greater tightness than actual skin, causing significant changes in the signal. The strain sensor implemented in the Skinsight™ apparatus quantifies alterations in current flowing through the sensor when the structure undergoes contraction or expansion, consequent to variations in charge within the ZnO. These changes are identified by a strain gauge, which is used to determine the magnitude of strain. In cases of contraction and expansion, the direction of current change is different as shown in Fig. 2(b). The presence of compressive strain, otherwise known as skin tightness, is indicated by an increase in current. During the experiment, the skin specimen undergoes a loss of moisture, accompanied by a continuous increase in tightness over the measurement period. As the experiment progresses, the skin specimen exhibits a loss of moisture and a concomitant increase in tightness over time. It is evident that when the loss of moisture is complete and the tightness phenomenon terminates, the increase in current stops. The graphs used in the data analysis process utilize a variety of analytical methods. In the case of normalization, tightness delay is evaluated by comparing the time values on the x-axis. In the regression results, tightness delay is determined by observing the slope of the graph, which gradually decreases in direction towards the lower right. Lastly, the area comparison graph is used to calculate the area of the upper surface of the graph, thus enabling a comparison to be made of the overall tightness delay effect of the product.

3.2. Verification of signal independence

For electronic sensors, even if they are designed to measure physical signals, significant changes to the signal may occur when they are in contact with moisture. In particular, given the high moisture content inherent in experimental specimens and cosmetics, it is imperative to verify the influence of moisture on the signal. The verification method involves a comparison of the direction of current change due to contraction of materials upon contacting water. Moreover, a comparison of the magnitude of current changes in response to both cases constitutes an additional method of verification. As mentioned in Section 3.1, the current increases when the material contracts, whereas it decreases when moisture comes into contact with it. Therefore, it can be concluded that these are distinct signals. Furthermore, it is evident that the magnitude of these changes indicates that the effects caused by pressure are approximately 1 %, while those caused by moisture can reach up to 10 times this value. This finding provides further support for the hypothesis that the forces measured are entirely different.

3.3. Feasibility assessment for statistical comparison

The manufacturing process of Skinsight™ involves a sophisticated semiconductor process, the purpose of which is to achieve a high level of detection performance. This process can lead to variations in sensor performance, even when minor changes are present. In order to

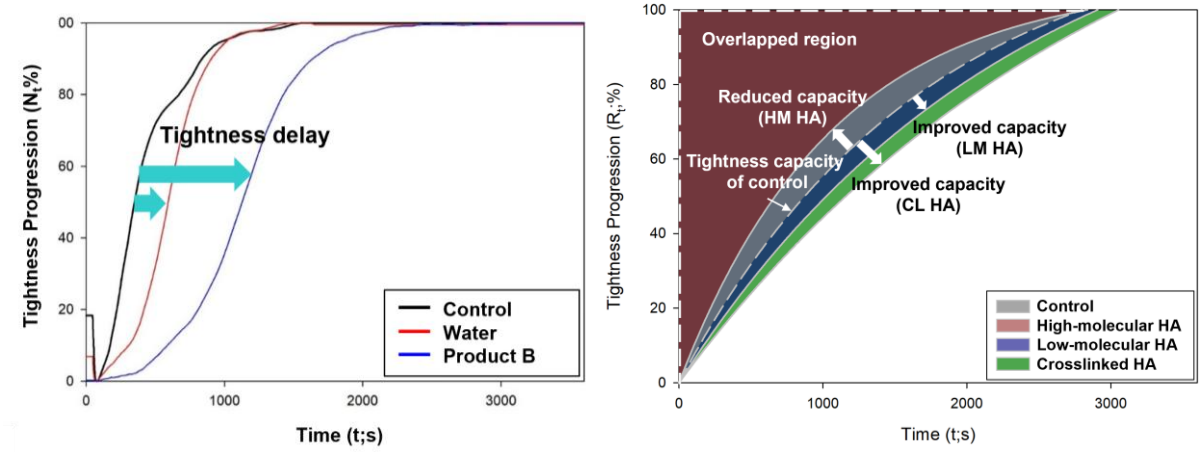

(**a**) (**b**)

Figure 4. *(a) Normalization results of stratum corneum permeation ability for Control, Water, and Product B. (b) Area comparison graph of the tightness delay effects according to the form of humectant for Control, high-molecular-weight hyaluronic acid (HA), low-molecular-weight HA, and crosslinked HA.*

address this issue, continuous improvements have been made to enhance the precision of the entire process. Furthermore, as mentioned in Section 2.3, emphasis has been placed on the consistent application of measurement protocols. Consequently, a reduction in the variation of initial current values to within 2 % was achieved, as demonstrated. Furthermore, sensors exhibiting deviations exceeding 5 % were not utilized in the experimental setup. Maintaining the standard deviation of the control group within 5 % consistently allows the tightness delay effect of the product to be regarded as significant, provided that the mean is at least 5 % greater than the lowest value of the standard deviation (for instance, if the standard deviation of the product is 10 %, the relative tightness delay capacity of the product must be 15 % or more). It is imperative that the product successfully penetrates the SC and is absorbed, and that its capacity for moisturization is validated through clinical test. Product B has been demonstrated to successfully penetrate the SC through tape stripping, and its formulation has been clinically verified to have moisturizing efficacy. Consequently, a clear delay in the progression of tightness over time was visually observed in Fig. 4(a) compared to the control.

4. Discussion

In order to prevent or delay skin tightness, it is important to consider the following approaches:

- The application of moisturizer to the skin
- The enhancement of the skin's mechanical resistance
- The restoration of the skin barrier function

In the context of these factors, the restoration of skin barrier function is difficult to observe in short-term tests, and increasing the skin's mechanical resistance is not significantly effective with cosmetics. The most frequently cited element in cosmetic improvements is moisturization, which is also the most effective against skin tightness. The mechanisms underlying moisturization are diverse and include direct water supply, occlusive effect and humectant

effect. The occlusive effect acts on the SC, while direct water supply requires penetration into the SC to be effective. In addition, it is imperative that humectants penetrate the skin in order to be effective. In the event that they are unable to pass through the SC, they may instead absorb moisture from the skin surface and thereby accelerate skin tightness. The in-vitro evaluation method for the tightness delay effect, including Skinsight™, not only evaluates the comprehensive tightness delay effect of products containing dozens of ingredients but also verifies whether it can assess the skin absorption of moisturizing ingredients and the effectiveness of individual ingredients such as humectants.

4.1. Discriminative capability for skin permeation (via SC)

The in-vitro test proposed in this study measures skin tightness by attaching a sensor to the bottom of the epidermis using a skin specimen, as an alternative to inserting a sensor into the skin. This method has the advantage of being able to accurately measure skin tightness and distinguish between different effects on the tightness delay depending on the SC permeability of the product under investigation. In order to verify this hypothesis, we tested the tightness delay effect of an untreated control group, pure water, and Product B, which exhibited a clear difference in SC penetration. Consequently, the application of water proved to be ineffective in comparison to the control group, while Product B exhibited a significant delay in tightness (Fig. 4(a)). This verified that the in-vitro test proposed is a system that can distinguish between differences based on skin permeation.

4.2. Evaluation of Humectant Effect Differentiation

In the field of cosmetics, hyaluronic acid (HA) is the most prevalent humectant. As mentioned above, HA has the capacity to attract and retain moisture from the ambient environment. However, its location can influence its effect on tightness. In order to verify the capacity of the in-vitro test to distinguish between these effects, low-molecular HA, which is easily absorbed into the skin [9], high-molecular HA, which is difficult to absorb [10], and crosslinked HA, known for its enhanced moisture-retaining properties [11], were applied and the results were examined. The crosslinked HA applied in this study was reduced to a nanoscale size for the purpose of facilitating its absorption by the skin. As demonstrated in Fig. 4(b), high molecular HA was found to accelerate tightness, as indicated by a decrease in tightness delay capacity. It has been observed that low-molecular HA appears to delay tightness, an effect attributable to an augmented capacity, with crosslinked HA demonstrating an even more enhanced tightness delay effect attributable to a more significant capacity increase in comparison with low-molecular HA. This outcome serves to validate the performance of our in-vitro setup, demonstrating its capability to facilitate the evaluation of the moisturizing properties of the raw materials.

Table 1. Calculation results of the tightness delay capacity and the relative tightness delay effects for Control and Product A to D, respectively

Variables	Control	Product A	Product B	Product C	Product D
Tightness Delay Capacity	78,625	82,749	164,532	91,059	104,588
Tightness Delay Effect	-	5%	109%	16%	33%

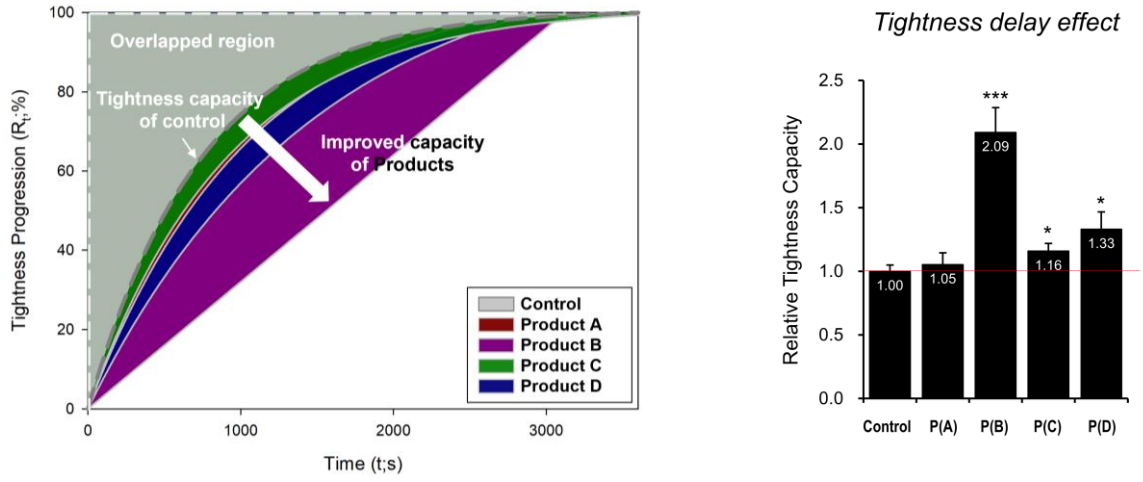

(**a**) (**b**)

Figure 5. (a) Area comparison graph of the tightness delay effects for Control and Product A to D; (b) t-test results for products, expressed as mean ± standard deviation (n = 3). Statistical significance levels were indicated as *p < 0.05, **p < 0.01, and ***p < 0.001 compared with the untreated control.

4.3. Comprehensive evaluation of tightness delay effect

In order to enhance the distinction between the products, a comparative analysis was conducted between products belonging to the same product category (serum), with the objective of identifying any significant variations. The selected products have been shown to have comparable viscosity and oil content, and are renowned for their tightness delay efficacy. As mentioned in Section 3.1, the larger area of the graph indicates that the greater potential capacity to delay tightness. Consequently, the tightness delay capacity and the relative tightness delay effects are represented in Fig. 5(a and b) and the values were calculated as shown in Table 1. In conclusion, it has been confirmed that the in-vitro setup can demonstrate sufficiently significant comparative differences even within the same product group (serum). This evaluation method is significant because it provides a comprehensive assessment of products containing various raw materials that influence skin tightness, taking into account the SC permeability and negative effects of ingredients, thereby enabling simple comparisons.

5. Conclusion

The in-vitro evaluation system developed in this study enables direct measurement of inner skin tightness by affixing the Skinsight™ ultra-sensitive strain sensor to the basal layer of a human ex-vivo epidermal model, minimizing signal loss during moisture evaporation-induced shrinkage. A LDPE film substrate was employed to ensure uniform two-dimensional shrinkage without edge curling. Signal independence from moisture interference was validated, and strict standardization of the experimental protocol minimized variability across measurements. Data consistency was further secured through normalization and exponential regression analysis. The system demonstrated the capability to differentiate products based on SC permeability, verifying that products capable of penetrating the SC delayed tightness progression more effectively. Furthermore, the model distinguished humectant efficacy at the ingredient level, successfully differentiating low-molecular-weight, high-molecular-weight, and cross-linked hyaluronic acid based on their respective impacts on tightness delay.

A comparative analysis among similar serum formulations further confirmed the method's sensitivity and reproducibility, with statistically significant differences observed in relative tightness delay capacities. Collectively, the developed in-vitro system with Skinsight™ offers a robust and sensitive platform for evaluating inner skin tightness, providing valuable insights for cosmetic formulation screening, raw material selection, and claims substantiation.

6. References

[1] R. Bennett-Kennett *et. al.*, Sensory neuron activation from topical treatments modulates the sensorial perception of human skin, (2023), *PNAS Nexus*, 2(9).

[2] D. Lunter *et. al.*, Novel aspects of Raman spectroscopy in skin research, (2022), *Experimental Dermatology*, 31(9), 1311–1329.

[3] M. Green *et. al.*, "Normal" TEWL-how can it be defined? A systematic review, (2022), *Experimental Dermatology*, 31(10), 1618–1631.

[4] J. Møss, The effect of 3 moisturisers on skin surface hydration: Electrical conductance (Skicon-200), capacitance (Corneometer CM420), and transepidermal water loss (TEWL), (1996), *Skin Research and Technology*, 2(1), 32–36.

[5] L. M. Aiello *et. al.*, Evaluation of operational parameters for clinical evaluation of skin hydration by corneometry method, (2025), *Brazilian Journal of Pharmaceutical Sciences*, 61.

[6] E. N. Montano *et. al.*, Comparison of Tape-Stripping Platforms as Non-Invasive Solutions for Skin Biomarker Discovery, (2024), *Journal of Investigative Dermatology*, 2595-2598

[7] H. Yeon *et. al.*, Long-term reliable physical health monitoring by sweat pore-inspired perforated electronic skins, (2021), *Science Advances*, 7, eabg8459.

[8] S. Grégoire S *et. al.*, Use of a simple in vitro test to assess loss of chemical due to volatility during an in vitro human skin absorption study, (2019), *Skin Pharmacology and Physiology*, 32(3), 117–124.

[9] Y. A. Nashchekina and M. Raydan, Noninvasive penetration of 5 nm hyaluronic acid molecules across the epidermal barrier (in vitro) and its interaction with human skin cells, (2018), *Skin Research and Technology*, 24(1), 129–134

[10] M. Essendoubi *et. al.*, Human skin penetration of hyaluronic acid of different molecular weights as probed by Raman spectroscopy, (2016), *Skin Research and Technology*, 22(1), 55–62.

[11] L. Guo *et. al.*, Preparation and Properties of Hyaluronic Acid Hydrogel Modified by L-cysteine Hydrochloride, (2021), *IOP Conference Series: Earth and Environmental Science*, 651(4), 042022.